HYPERSPECTRAL INVESTIGATIONS OF MINE WASTE AND ABANDONED MINE LANDS – THE DRAGON CALIBRATION SITE CASE STUDY

Phoebe L. Hauff,[1] Douglas C. Peters,[2] Gary Borstad,[3] William Peppin,[1]
Eric Dillenbeck,[4] L. Graham Closs,[4] and Eric C. Prosh[1]

[1]Spectral International Inc.
P. O. Box 1027
Arvada, CO 80001
Email **pusa@rmi.net**

[2] Peters Geosciences
169 Quaker Street
Golden, CO 80401-5543

[3]G.A. Borstad Associates Ltd.
114-9865 W Saanich Road
Sidney, B.C. V8L 5Y8
Canada

[4]Colorado School of Mines
Golden, CO 80401

1. Introduction

The utilization of remotely sensed hyperspectral data for the evaluation of mine waste and the classification of abandoned mine lands (AML) is being advanced toward an operational, commercial technology. Partly through the auspices of the NASA EOCAP program (Project NAS-13-99004) and U.S. Environmental Protection Agency (EPA) AML programs, sites in Utah are under investigation using AVIRIS, SFSI, and CASI hyperspectral sensors. This paper presents a brief look at this study and discusses the methods used.

2. Overall Objectives of the Studies

The general objectives of the two linked NASA-EOCAP and EPA-AML projects are to satisfy the directives of both agencies to commercialize the investigation and monitoring of mine waste through the utilization of remote sensing techniques. The EPA and various other government agencies are making concerted efforts to evaluate the extent of environmental impacts from historic mining and to distinguish problem sites from innocuous sites. Conventional ground methods to find and evaluate wastes are too time consuming and expensive. Use of remote sensing is a possible answer.

The question to be addressed is, can this be done economically with present technology? Waste discrimination looks at subtle changes in mineralogy and waste materials. This means that smaller pixel size and finer spectral resolution are needed. However, this creates very large data sets. These large data sets have to be handled efficiently and rapidly. Processing has to be faster, more accurate, and consistent. New mineral identification algorithms must be developed.

One of the more important issues that are rarely addressed is accuracy assessment. This means detailed field checking with field spectrometers and X-Ray Fluorescence (XRF) when metals are involved.

3. Technical Objectives

It first must be understood what mine waste is from a remote sensing perspective and how it is possible to better identify, characterize, evaluate, and monitor it spectrally. This differs from conventional characterization ideas. Standardized protocols for commercial applications to mine wastes must be developed.

Data processing techniques are being further evaluated and new algorithms developed, as the information required for remediation is spatially very detailed.

4. General Outline of the Method

The method under development for mine waste evaluation involves the following tasks to achieve a final product of hyperspectral images and waste maps: 1) compilation of geologic background and historical information, 2) field reconnaissance, 3) airborne data acquisition, 4) analytical support (e.g., XRD, XRF, SEM), 5) integration of data sets, 6) image processing, 7) field checking of images, and 8) accuracy assessment.

4.1 Field reconnaissance is done before or at the time of airborne data acquisition. The following types of information are collected: 1) SWIR range reflectance spectra from rocks, soils, sediments, and vegetation, 2) solar spectra for reflectance calibration and vegetation spectra, 3) portable XRF chemical analyses of same, 4) digital and film photographs of sample sites, and 5) GPS coordinates for samples and control points.

4.2 Data from three sensors were used in these studies: AVIRIS, SFSI (SWIR Full Spectrum Imager) and CASI (Compact Airborne Spectrographic Imager). The AVIRIS is flown for NASA by the Jet Propulsion Laboratory, usually at an altitude of 65,000 ft. SFSI and CASI are flown by G.A. Borstad Associates at 10,000-12,000 ft. Table 1 compares the three hyperspectral sensors.

The ENVI software package was the main program used to process the data in this application. Hyperspectral **image processing** is still a relatively new subdiscipline. The production of high quality hyperspectral images is a process requiring numerous calibrations, calculations, and refinements.

Table 1. Airborne instrument configurations. AVIRIS data from Vane (1993).

	AVIRIS	SFSI	CASI
Band width	12 nm	10 nm	2-4 nm
Spectral range	400–2500nm	1220-2320 nm	403-1000 nm
FoV		35^o	35^o
Ground pixel size	17 m	4 m	4 m
Swath width	11 km	2 km	2 km

One of these refinements is integration into the images of spectral data from high-resolution field spectrometers. This allows a more precise determination of end-members for the program to map and use in “unmixing” algorithms. It also pre-supposes an understanding of local geology. The ideal situation would be to allow the computer program to search, identify, and classify all components of the image. In practice, this does not yet work effectively. When investigators have an idea of what is on the surface or what particular mineral or material is targeted, and spectra of the ground targets are available, processing will be more accurate.

Three different approaches were used to analyze these data and produce images of varying complexity. The first employed general processing techniques based more on the well-known Landsat methods. The raw data first were calibrated using proprietary programs. An IARR correction was applied to correct to relative reflectance. The image was warped to control points chosen from topographic maps, digital orthophotographs, and GPS points. It is not unusual to use hundreds of control points to correctly rectify an airborne image.

The initial images were created through a general processing technique, which chose contrasting bands to a target material band. This created a false-color image. The Crosta Landsat processing algorithm also was used to highlight the iron minerals. These two images provide a coarse idea of what materials are present and their distribution.

This was followed by classification procedures. These are done with a less conventional approach using field spectral data collected before image processing starts and then integrated with the images. Finally, to validate this technique, the "pure pixel end member" method was implemented (Boardman, 1993).

4.3 Accuracy assessment of the processing and classification results is performed by revisiting the study area and performing test traverses and sampling across key areas of identified classes. The predictive capabilities of the images and classes are evaluated against mineralogy and metal contents within the context of the field and geological conditions (such as sedimentation and erosion along streams).

5. Dragon Mine Case Study

5.1 Background

The Dragon Mine case study is part of the NASA EOCAP and EPA Utah AML studies. This mine is a large clay deposit in the Tintic District in central Utah (Figure 1). The Dragon Mine was chosen by EPA study participants as a common reference site where field calibration data could be collected to ground truth AVIRIS and other images. The mine site and wastes visually appeared to have potential as an acid drainage generator.

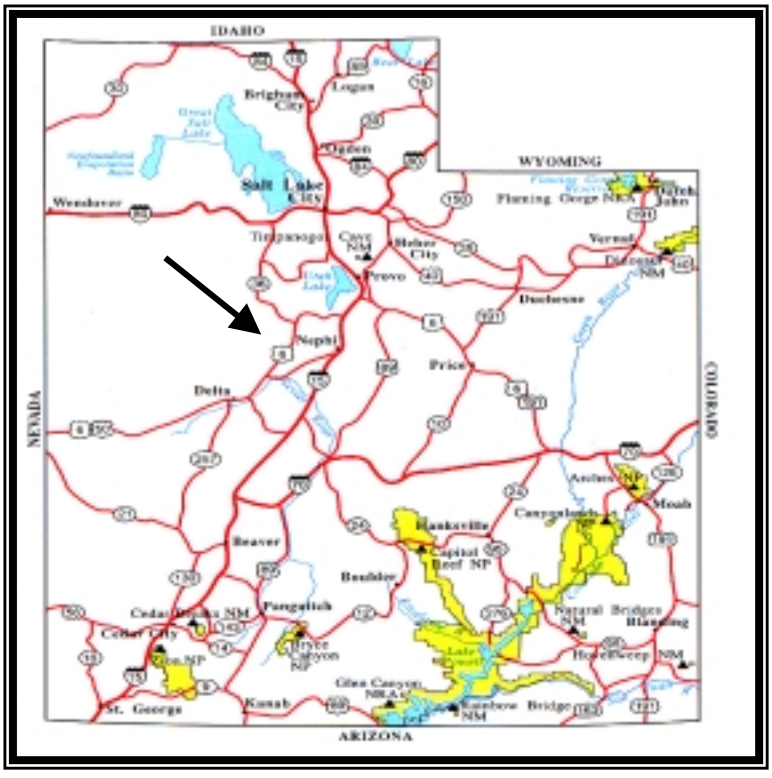

Figure 1 – Location map for the Dragon Mine.

The Dragon, discovered in 1870, was the second mine in the historic Tintic district. The initial workings were in small Au-Ag-Cu-Pb veins. Later the abundant iron oxide ores were mined as flux for smelting. In 1938, the clay mineral halloysite was identified by X-Ray diffraction. By 1949, the Filtrol Corp. had patented halloysite as a

catalyst for petroleum cracking and mined the Dragon until 1976 when a synthetic catalyst was developed to replace the natural halloysite.

This deposit is a halloysite, kaolinite, and iron oxide replacement body developed along the Sunbeam-Dragon Fissure Zone, which is a north-northeast trending structure about 150 m wide (Morris, 1985). This zone lies on the contact between the Silver City monzonite porphyry stock and the marbleized Ajax Dolomite of late Cambrian age. Alteration mineralogy at the Dragon includes halloysite (both 10 A° ("endellite") and 7 A° (dehydrated) phases), kaolinite (well-ordered, poorly ordered and amorphous allophane, and the silica-rich variety anauxite). Other minerals include alunite, illite, smectites (montmorillonite and nontronite), and carbonates (calcite and dolomite). There is minor jarosite, pyrite, gypsum, phosphate, and gibbsite.

There were five alteration stages in the Tintic District. The Dragon deposit was emplaced during the second or "argillic alteration" stage. This was pre-mineralization, pre-pyritization, and pre-sericitization alteration. Therefore, there are minimal sulfur and potassium sources available for acid generation in this deposit. The Dragon deposit was formed by contact metasomatism along the Dragon Fissure Zone. This means that the dolomite host was replaced, volume for volume, with hydrous aluminum silicates or clays through the action of hot hydrothermal fluids. Massive iron oxides and minor iron-smectite (nontronite) were emplaced along the carbonate rock contact.

The Dragon is an excellent illustration of a site with the visual potential of AMD (acid mine drainage), as it is very oxidized and it has been suggested there is jarositic alteration. There is, however, no acid drainage problem at the Dragon. Although the mine dumps show strong yellow coloration, this is limonitic iron (oxide), not jarositic (sulfate). Jarosite occurs only locally and is a product of minor disseminated pyrite from post-Dragon deposit alteration. There also are very low contents of heavy metals. The small base metal veinlets exploited at the turn of the century did not yield significant metals. The semi-arid climate does not provide sufficient ground water activity to move appreciable amounts of metals into the drainages. Figure 2 shows the distribution of ground samples containing jarosite. There are only 15 out of the over 100 samples collected. The PIMA™ spectrometer and later the hyperspectral images were able to demonstrate the differences between the more hazardous acid and more benign neutral systems.

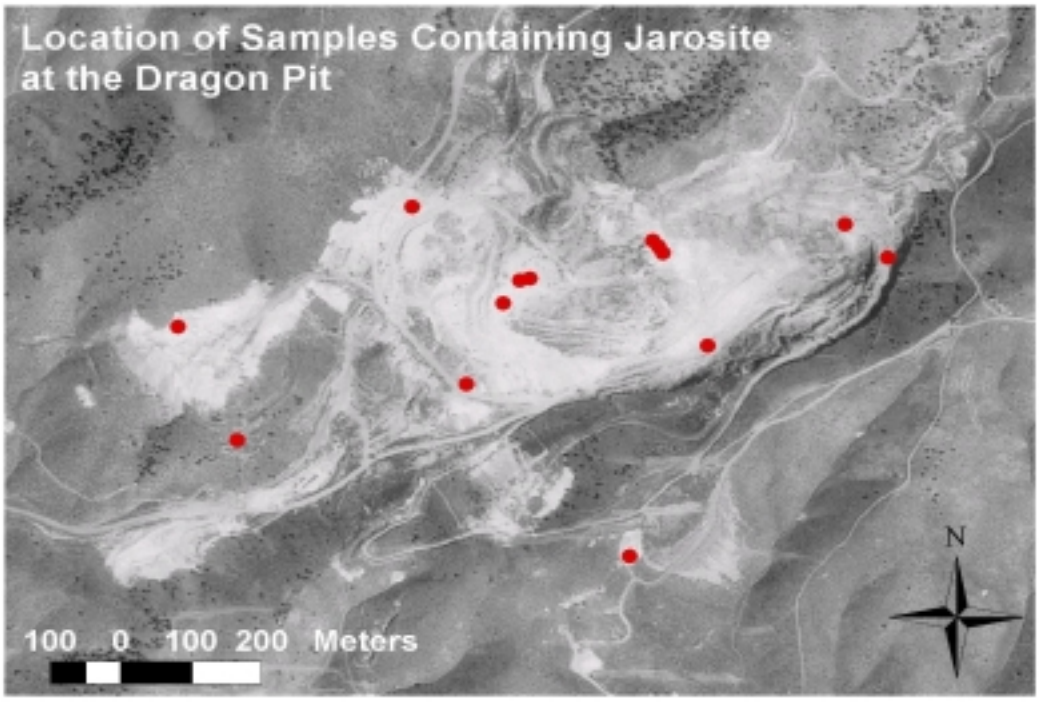

Figure 2 – Sample map, overlain on an orthophoto, of jarosite containing samples.

5.2 AVIRIS Images

Both AVIRIS and SFSI images were acquired and processed over the Dragon area. Figure 2 shows an AVIRIS false-color image of most of the Tintic District. The pale blue areas highlight alteration at the mines and other clay-bearing outcrops. Vegetation in green and red indicates scrubland, grassy areas, and slopes. The district extends from the town of Eureka (E) to the south and east. The Dragon (arrow) is in the south central part of the image. This image was processed by Alistair Lamb.

The AVIRIS classification image in Figure 3 is an alunite map centered around the Dragon Mine. There is very little alunite displayed at the Dragon with the 20m pixel resolution. This image was processed by Alistair Lamb using the Hypips program.

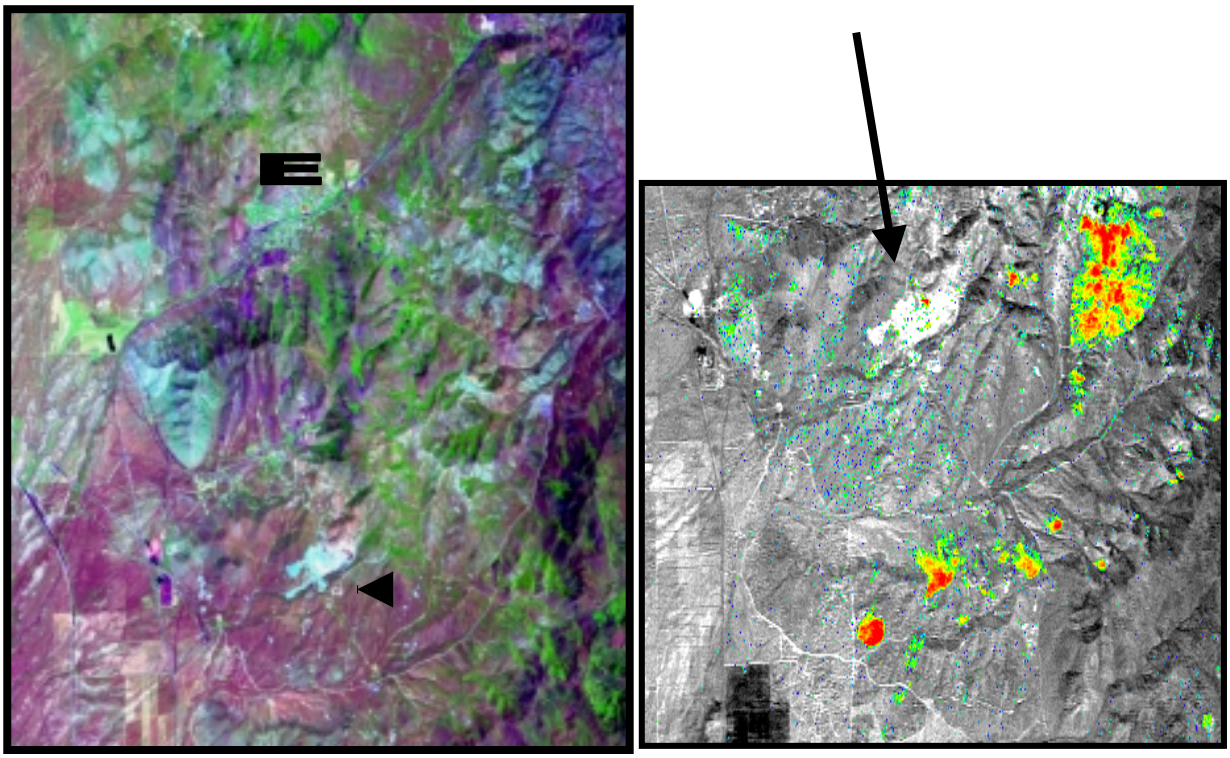

Figures 3, 4 – Left to right: AVIRIS RGB and AVIRIS Alunite classification images, Tintic District. Dragon is indicated with an arrow.

5.3 Spectra –SFSI

The major constituent minerals found at the Dragon Mine are shown in Figure 5 in a compilation of end member spectra from the SFSI images. These species were first identified with PIMA on the ground and then extracted from the images.

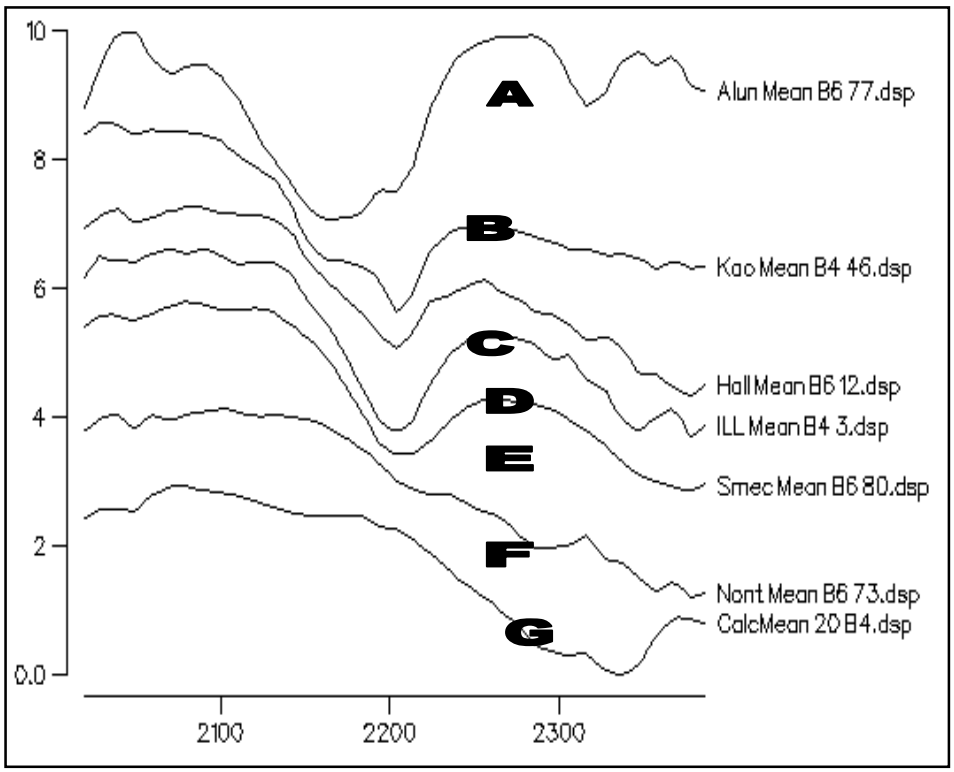

Figure 5 – End member spectra from the SFSI images. Spectra have been averaged with several pixels combined per spectrum and include alunite [A], kaolinite [B], poor halloysite [C], illite [D], smectite [E], nontronite [F] and calcite.[G]. These are very good examples of the mineral spectra and correspond well to PIMA reference spectra.

Alunite is only sparsely distributed at the Dragon, however, it is important in the paragenesis of the mine. Compare Figure 6, a ground sample map for alunite, with Figure 7, the SFSI image for alunite. Note that all the alunite ground sample locations are correlated to the image.

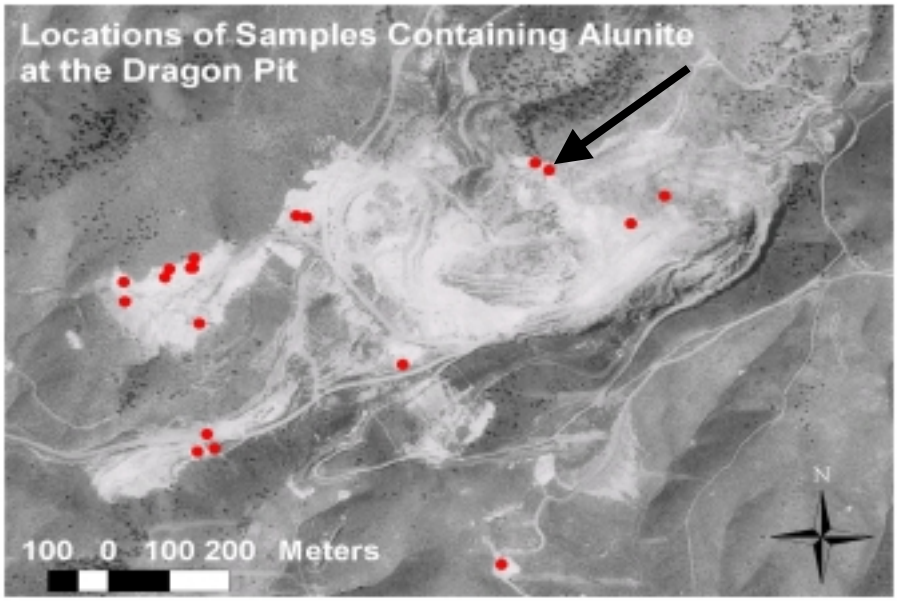

Figure 6 – Distribution of alunite-bearing ground samples at the Dragon (1998 only) identifications. This image is a particularly good example of the high resolving capabilities of the SFSI sensor. Arrow indicates Dragon Fissure.

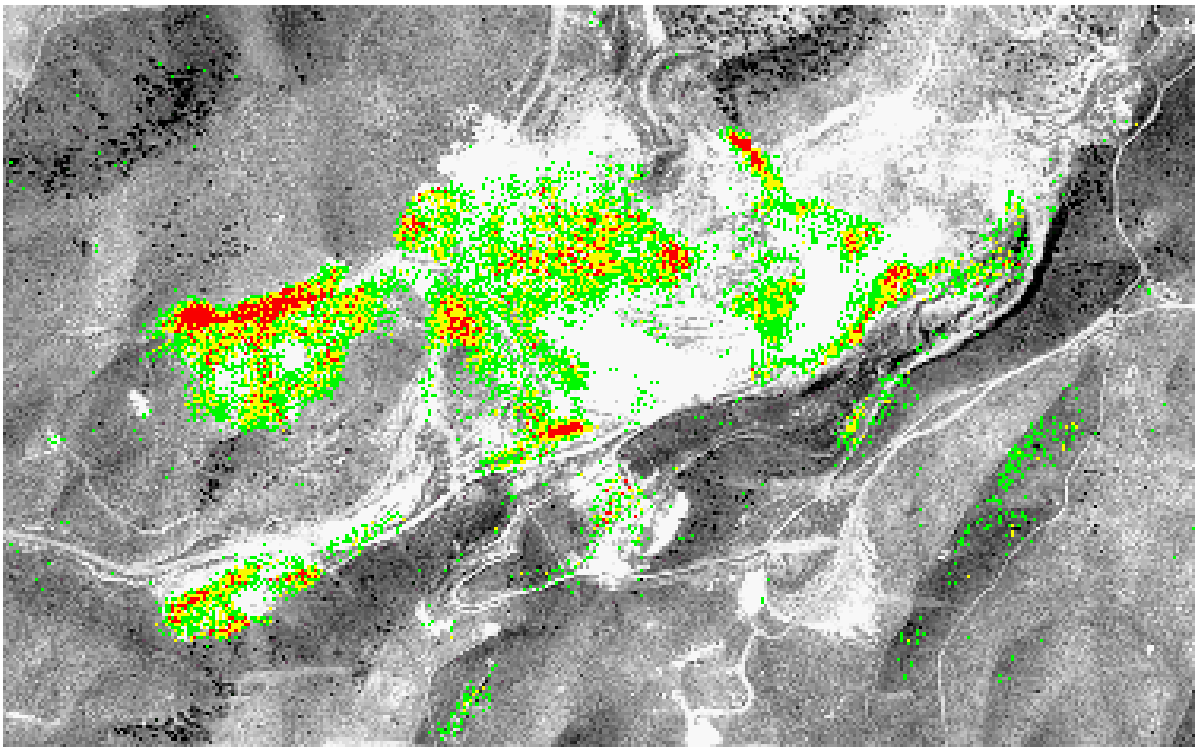

Figure 7 – SFSI Subset of Figure 3 (alunite image) showing the Dragon Mine. The red pixels have the highest confidence, then the yellow and then green.

The SFSI sensor was able to discriminate the alunite along the narrow structures in the Dragon Fissure Zone (arrow), which is shown in the sketch in Figure 8. This type of detail is not seen as well in the high altitude AVIRIS images and is very important for exploration and environmental applications for identifying source and differentiating waste from unaffected materials.

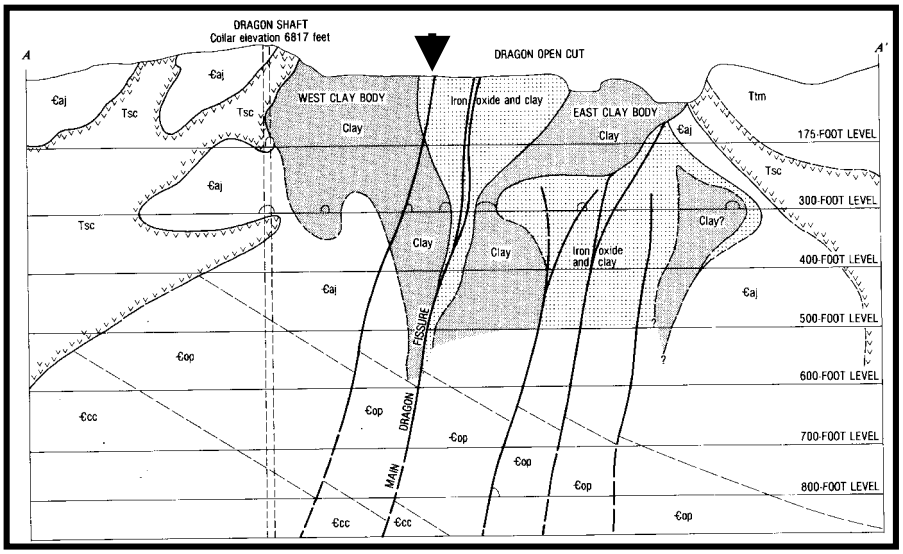

Figure 8 – Sketch cross section of the Dragon Mine. The Dragon Fissure is indicated with an arrow (Morris, 1985).

The SFSI image in Figure 9 shows the distribution of the kaolinite group minerals through the pit. This includes kaolinite (both poorly crystalline and well crystalline), kaolinite overprinting illite, and both 7 and 10 A° halloysite. As would be expected, these minerals dominate the pit walls and dumps.

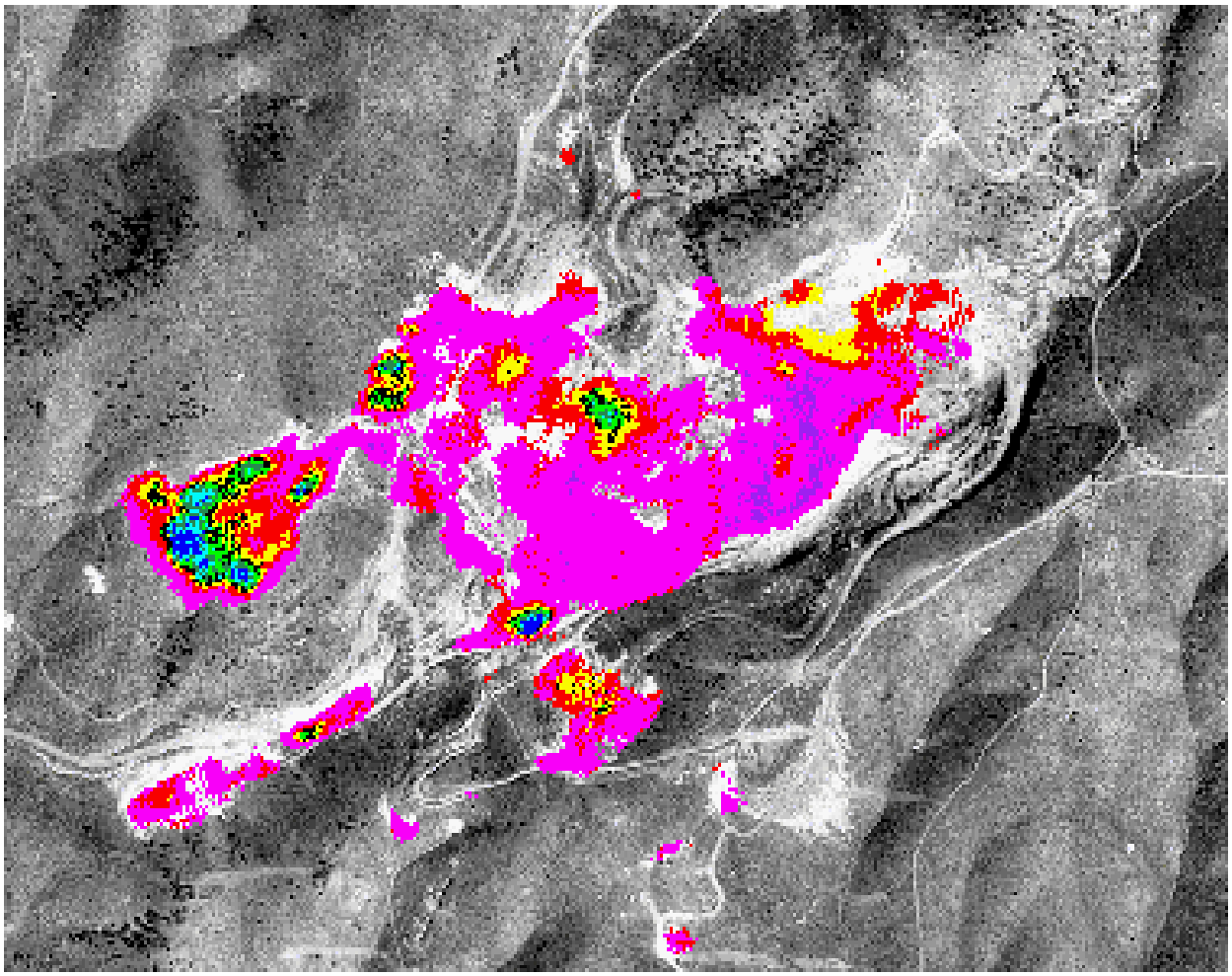

Figure 9 – This SFSI image shows a progression from end member halloysite to end member kaolinite through several stages. The color key is halloysite purple->magenta->red-yellow->black (equal) -> sea green ->green->cyan->blue end member kaolinite.

These minerals have very similar chemistry and crystal structure and therefore very similar spectra as can be seen in Figure 10, which plots SFSI spectra extracted from the image. This is a unique plot because it shows more then just differences between closely related mineral species. It actually shows subtle differences in the octahedral layer configurations of these minerals.

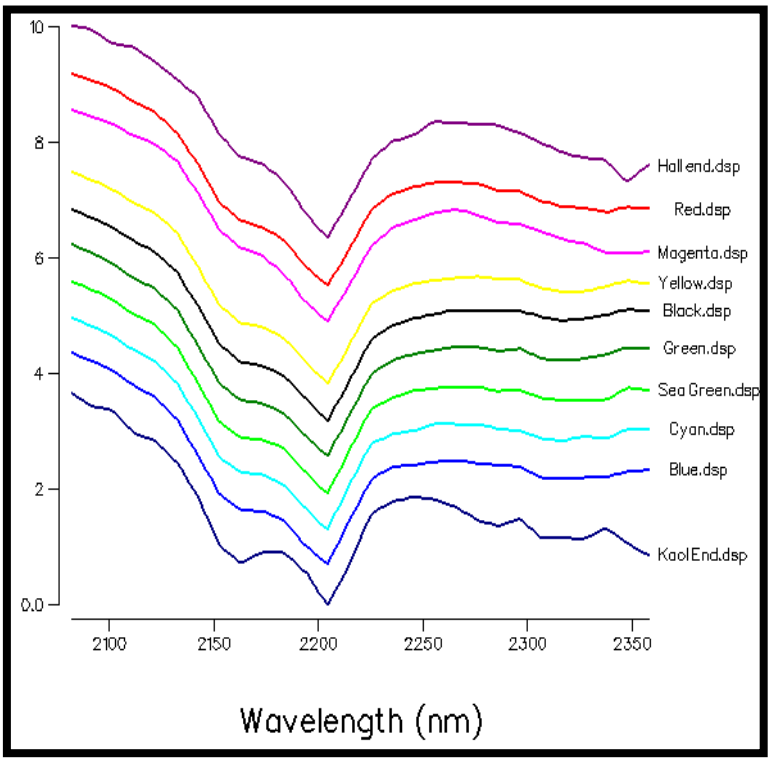

Figure 10 – SFSI spectra extracted from the image shown in Figure 9 where the halloysite end member is shown on the top of the stack in purple and the kaolinite end member in blue on the bottom of the stack.

The Dragon Case Study illustrates well the capabilities of remote sensing technology for the evaluation of mine lands. It demonstrates the ability of the SFSI sensor to discriminate between transitional phases that are actually sub-mineral, on the octahedral layer level. The SFSI system is excellent for this work because of its fine detail in both spectral and spatial. The Dragon example also shows that the differences between acid and neutral pH drainage systems can be determined using hyperspectral airborne data

6. References

Boardman, J., 1993. Automatic spectral unmixing of AVIRIS data using convex geometry concepts, *in* Proceedings of the Fourth Annual JPL Airborne Geoscience Workshop, JPL Publication 93-26, Vol. 1, 25-29 October, 1993.

Morris, H.T., 1985. Geology, ore bodies and halloysite deposits of the Tintic Mining District, pp. 40-53, *in* Field trip Guidebook, Clay and Clay Minerals, Western Colorado and Eastern and Central Utah. 1985 International Clay Conference, Denver Co, July 28-August 2, 1985.

Vane, G., et al., 1993. The Airborne Visible/Infrared Imaging Spectrometer (AVIRIS): Remote Sensing of Environment, 44: 127-143.